



IJRASET

International Journal For Research in
Applied Science and Engineering Technology



INTERNATIONAL JOURNAL FOR RESEARCH

IN APPLIED SCIENCE & ENGINEERING TECHNOLOGY

Volume: 5 Issue: XI Month of publication: November 2017

DOI: <http://doi.org/10.22214/ijraset.2017.11032>

www.ijraset.com

Call:  08813907089

E-mail ID: ijraset@gmail.com

Effect of Filler Composition and Post Weld Heat Treatment on Mechanical and Metallurgical Properties of GTA Welded AISI 409M Stainless Steel Joints

Neeraj Vishwakarma¹, Mandeep Singh², Amandeep Singh³

^{1, 2, 3} Department of Mechanical Engineering, CT Institute of Engineering, Management and Technology, Shahpur, Jalandhar, Punjab, India

Abstract: The effect of filler composition and post weld heat treatment on mechanical and metallurgical properties of Gas Tungsten Arc welded AISI 409 Stainless Steel was studied. Rolled plates of 4mm thickness have been used as the base material for preparing double pass one is root pass and second is cover pass butt welded joints. Welding of ferritic stainless steel plate has been performed in three phases. During 1st phase of welding, 409M ferritic stainless steel with similar filler metal is used at direct current of 100A, during 2nd phase of welding of base plates by using 309L austenitic stainless steel filler metal is used and during 3rd phase of welding, 410 martensitic stainless steel filler metal is used at a direct current. Maximum UTS value of welded joints possessed by the welded joints which is fabricated with 409M filler, maximum Impact strength value possessed by the welded joints which is fabricated with 309L, and maximum average hardness is recorded in WJ₂ (342VHN) in as-welded condition. Grain coarsening effects was revealed in the microstructures images that had been taken by the optical microscope in all the welded joints after PWHT as compared to the microstructure images of welded joints in as-welded condition.

Keywords: AISI 409M, welded joints, filler material, mechanical & metallurgical properties, PWHT.

I. INTRODUCTION

Ferritic stainless steels are known for their excellent stress corrosion cracking resistance and in chloride environment; it shows good resistance to pitting fissure corrosion [1]. They are commonly utilized under a severe corrosion atmosphere for chemical processing equipments, furnace parts, heat exchangers, oil burner parts, petroleum refining equipment, protection tubes, storage vessels, electrical appliances, solar water heaters and house hold appliances. They are cheaper alternatives to austenitic stainless steels [2]. No doubt, in wrought conditions these alloys possess useful properties, welding is known to reduce their toughness, ductility, and corrosion resistance, because of coarsening and formation of martensite. Due to these factors, there is some limitation in the application of this group of alloys [3]. The problem of excessive grain growth can be overcome by using lower welding heat inputs. To suppress the grain growth it has also been suggested that nitride and carbide formers such as B, Al, Zr and V can be added to the ferritic stainless steel [4]. Nickel supports the rate of formation of passive film. At the point when Ni is included sufficient amount, it balances out the austenitic phase. It gives toughness, ductility and ease of weldability. Since Ni is costly, Steel Authority of India (SAIL) created Stainless steel called 409M with ideal level of Ni and Cr content. These elements give essential corrosion resistance and are more affordable when contrasted with different evaluation of stainless steel [5]. It was developed from ferritic stainless steel AISI 409 by careful balancing of ferritic (Cr, Si, Ti) and austenitic (Ni, Mn, C, N) stabilizing elements using Kaltenhauser's relationship in following Equation

Kaltenhauser Ferrite Factor (KFF)

$$= Cr + 6Si + 8Ti - 2Mn - 4Ni - 40(C+N)$$

On cooling, it transforms partially to austenite from ferrite which enhances the weldability properties and as-welded toughness by restricting heat affected zone (HAZ) grain growth, passing through the dual phase austenite-ferrite phase on the Fe-Cr equilibrium phase diagram in Fig. 1 [6].

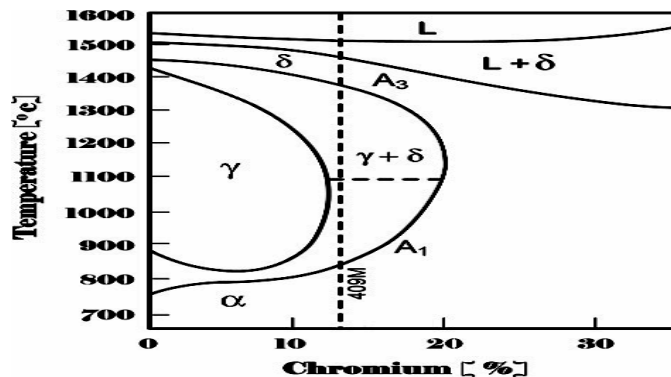


Fig. 1: Fe-Cr equilibrium phase diagram showing the position of 409M ferritic stainless steel [6].

The sensitization range for ferritic stainless steels lies above 925°C, and immunity to intergranular corrosion is restored by annealing in the range of 650-815°C for about 10-60min [7]. It is observed that when ferritic stainless steel is welded by using Gas Tungsten Arc Welding (GTAW) process, the equiaxed fraction values depends on the welding speed, it is increased with welding speed, for the second phase the nucleation was formed because of presence of titanium and aluminum for constant values of heat input per unit distance. Tin quenching of GTA welds of commercial ferritic stainless steel had indicated heterogeneous nucleation of equiaxed grains on tin particles in front of progressing columnar interfaces. However, the addition of titanium alone did not prompt the development of equiaxed grains, in spite of an increased tendency for branching and protrusion of some primary stalks ahead of others [8]. Mohandas et al. [9] did comparative evaluation of GTA and Shielded metal arc (SMA) welds of AISI 430 stainless steel and observed that GTA welds had greater ductility and strength as compared to those of SMA welds. Impact properties of the heat affected zone are influenced by the carbon and nitrogen contents in 11-12% chromium steel [10]. Mechanical properties like ductility, hardness, yield strength and impact resistance can be enhanced by using heat treatment process for carbon steel. The electrical, corrosion and thermal conductivity are also slightly changed amid heat treatment process. The standard qualities of steel utilized as a part of the basic outline are recommended from their yield strength. Most building estimations for structure depend on yield strength [11]. Ample of work has been done on the 409M ferritic stainless steel about their mechanical behavior and up to what extent these properties depend upon input parameters. Few research papers investigated the effect of filler metal on mechanical and metallurgical properties of AISI 409M. But the published information on the effect of filler composition and PWHT on the mechanical and metallurgical properties of AISI 409M is not available. Hence, to fulfill the gap the present investigation carried out.

II. EXPERIMENTATION

A. Welding

The as-received base material (BM) used in this experiment was 4mm thick cold rolled and annealed AISI 409M grade ferritic stainless steel plates with dimension of 300mm×100mm. The chemical compositions of base metal and filler metals are presented in Table 1. Tack welding is used to secure the plates in position for getting initial joint configuration. Single ‘V’ butt joints were fabricated using GTA welding process with 309L, 409M and 410 filler metals. Necessary care was taken to avoid joint distortions and weld joints made by using clamping device. The welding conditions and process parameters used to fabricate the joints are given in Table 2. The welded joint was sliced by power hacksaw and then machined to the required dimensions for preparing tensile, impact, hardness and microstructure test specimens as shown in Fig. 2.

TABLE 1: Chemical composition of filler metals (wt%)

Elements	C	Mn	Cr	S	Si	Ni	P	Fe
409M(BM)	0.026	1.09	10.93	0.01	0.38	0.40	0.029	Balance
309L	0.20	2.00	23.00	0.03	1.00	14.00	0.04	Balance
409M	0.026	1.09	10.93	0.01	0.38	0.40	0.029	Balance
410	0.15	1.00	13.50	0.03	1.00	0.75	0.04	Balance

TABLE 2: Welding Parameters for 1st, 2nd and 3rd Phase of Experiments

Sr. No	Phase	Filler Metal	Pass No.	Welding Current (I) amp.	Arc Voltage (v) volts	Welding Speed (s) mm/sec	Heat Input (kJ/s)	Total Heat Input (kJ/s)
1	First Phase	309L	Root pass	100	13	1.56	0.66	1.21
			Cover pass	100	13	1.87	0.55	
2	Second Phase	409M	Root pass	100	13	1.49	0.69	1.29
			Cover pass	100	13	1.71	0.60	
3	Third Phase	410	Root pass	100	13	0.92	1.13	1.96
			Cover pass	100	13	1.25	0.83	

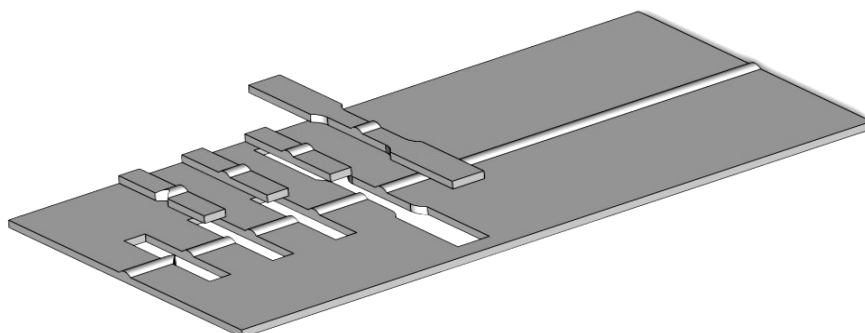


Fig. 2: Extrusion of Specimens for Mechanical Testing and Metallurgical Testing

Tensile test was conducted by using universal testing machine (UTM). ASTM E8M-04 guidelines were followed for preparing and testing tensile specimens. Impact test was conducted at room temperature using pendulum type impact testing machine. ASTM E23-04 specifications were followed for preparing and testing the specimens. The actual photograph of the fractured tensile specimen is shown in Fig. 3.

Vickers Micro-hardness testing machine was employed for measuring the hardness of the test specimens. Micro-structure examination was carried out by using light optical micro-structure incorporated with image analyzer software. Required size of micro-structure test specimens were extracted from the welded piece and were polished using different grades of emery papers. After this last stage polishing was done by using the diamond compound in the disc polishing machine. The extracted and polished test specimens were etched with 5 ml hydrochloric acid, 1g picric acid and 100ml methanol applied for 10-15s. The dimensions of mechanical and metallurgical test specimens are shown in Fig. 4.

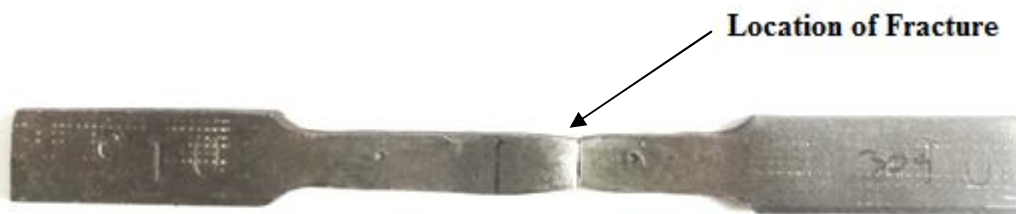


Fig. 3: Actual photograph of the fractured tensile specimen

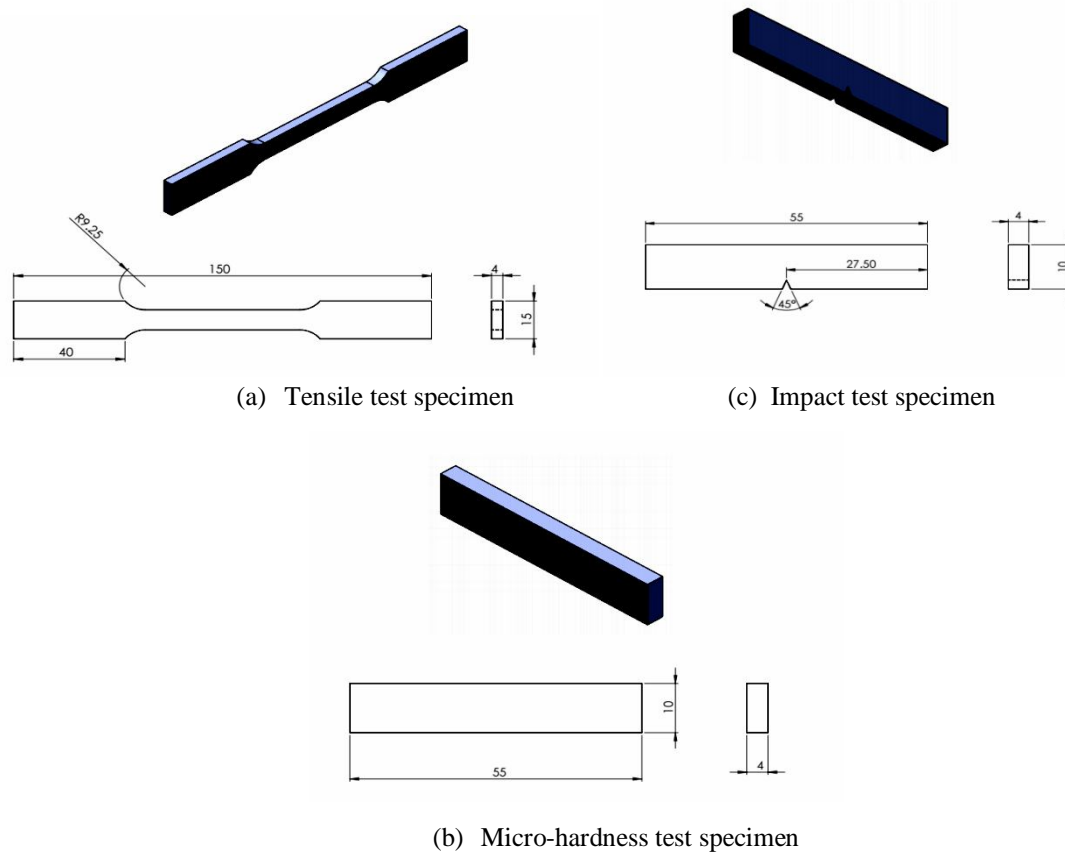


Fig. 4: Dimensions of Mechanical and Metallurgical Test Specimens

B. Post Weld Heat Treatment

790°C temperature was used for PWHT of 409M ferritic stainless steel followed by soaking/holding for 60 minutes to prevent further grain coarsening. Furnace cooling is used for the cooling purpose. In furnace cooling there is a slow cooling in which the furnace is switched off for 24 to 48 hours.

III. RESULTS

To acquire the appropriate results, a series of experimentation was performed on the welding set up in three phases by using different filler metals as discussed in chapter 3 for carrying out the mechanical and metallurgical testing to achieve objectives. The results are presented in graphs and table form

A. Tensile Properties And Impact Properties

To get tensile transverse properties such as tensile strength and percentage elongation, tensile test was carried out in UTM on the extruded test specimens from the welded joints. Three specimens were tested in as welded conditions and rest three specimens were tested in post weld heat treated conditions. The average of three results of transverse tensile test is listed in Table 3. The fracture was occurred at base metal which is shown in Fig. 3 that directly means the strength of weld metal is stronger than the base metal. The percentage elongation of the weld joint developed by the PWHT specimens are higher than that of the as-weld specimens irrespective of filler metals. On comparing among WJ₁ (welded joint fabricated using 309L filler metal), WJ₂ (welded joint fabricated using 409M filler metal), and WJ₃ (welded joint fabricated using 410 filler metal), WJ₂ joint has highest tensile strength as it shows 10% and 9% stronger than WJ₁ and WJ₃ joints in as-welded condition and for PWHT condition WJ₂ shows 8% and 18% stronger than WJ₁ and WJ₃, respectively. Charpy impact toughness values of all the joints were evaluated and they are presented in Table 4. Of the three joints, the WJ₁ exhibited higher impact toughness values, and the enhancement in toughness value is approximately 32% compared to WJ₂ and 12% compared to WJ₃ in as-welded condition and for PWHT condition WJ₂ exhibited 22% and 7% compared to WJ₁ and WJ₃, respectively. After PWHT there is increment in the values of impact toughness. There is 25%, 40% and 32% increment for WJ₁, WJ₂ and WJ₃ in as welded condition compared to PWHT condition.

TABLE 3: Tensile Property of GTAW Joints

Specimens (Filler Metal)	Results				Location of fracture
	As-welded (MPa)	Elongation As welded (%)	After Post weld Heat Treatment (MPa)	Elongation After Post weld Heat Treatment (%)	
WJ ₁ (309L)	490.89	9	470.10	11	Base Metal
WJ ₂ (409M)	550	5.6	511	6.2	Base Metal
WJ ₃ (410)	500	6.66	415	7.5	Base Metal

TABLE 4: Impact Property of GTAW Joints

Specimens (Filler Metal)	Results	
	As welded	After Post weld Heat Treatment
WJ ₁ (309L)	32 J	40 J
WJ ₂ (409M)	22 J	31 J
WJ ₃ (410)	28 J	37 J

B. Hardness and Microstructure

Vickers Micro-hardness value of the welded zone has been measured for all the welded specimens at the cross-section to understand the change in mechanical property of the welded zone. In Fig. 5, Fig. 6 and Fig. 7, “0” indicates the center of fusion zone and show the Vickers Micro-hardness value at the welding zone taken from the centre of the welding zone towards the base materials for different samples which were fabricated by the different filler metals. The average values of Vickers Micro-hardness tests are enlisted in Table 5. From the graph it is found that for almost all the sample Vickers Micro-hardness value increases in the welding zone irrespective of filler metal than the base metal and HAZ these values are in the range of 327VHN to 415VHN in the welded zone. After some distance away from the welded zone these values start decreasing to the hardness of the base material for the sample. The optical images of WJ₁, WJ₂ and WJ₃ are shown in Fig. 8 (a), (b) and (c) respectively in as-welded condition. Fig. 8 (d), (e) and (f) show the optical images of WJ₁, WJ₂ and WJ₃ in PWHT condition

TABLE 5: Average Vickers Micro-hardness Value of GTAW Joints

Specimens (Filler Metal)	Results	
	As welded(VHN)	After Post weld Heat Treatment (VHN)
WJ ₁ (309L)	318	262
WJ ₂ (409M)	342	307
WJ ₃ (410)	326	260

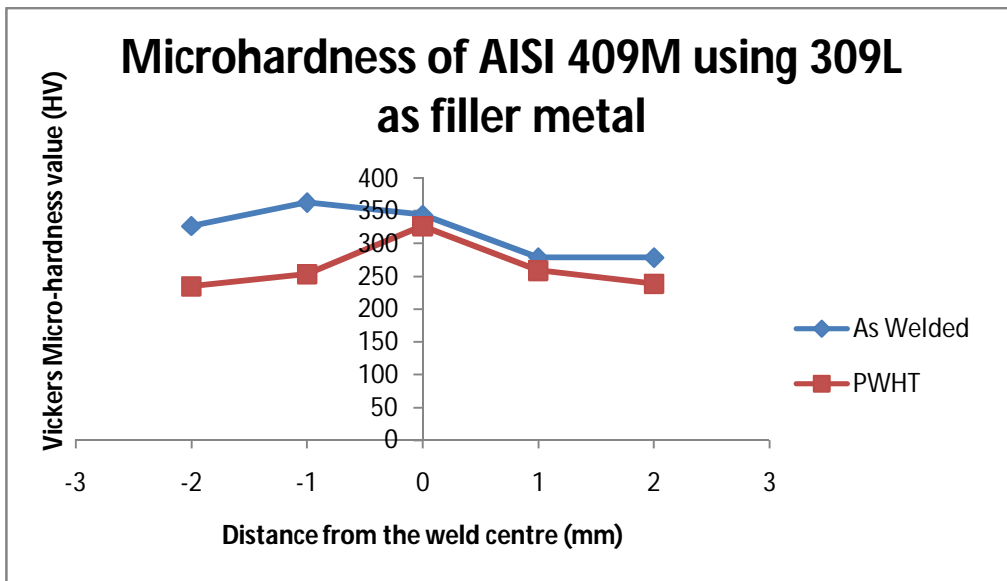


Fig. 5: Hardness Profile of GTAW Joints of SS409M Using 309L as Filler Metal.

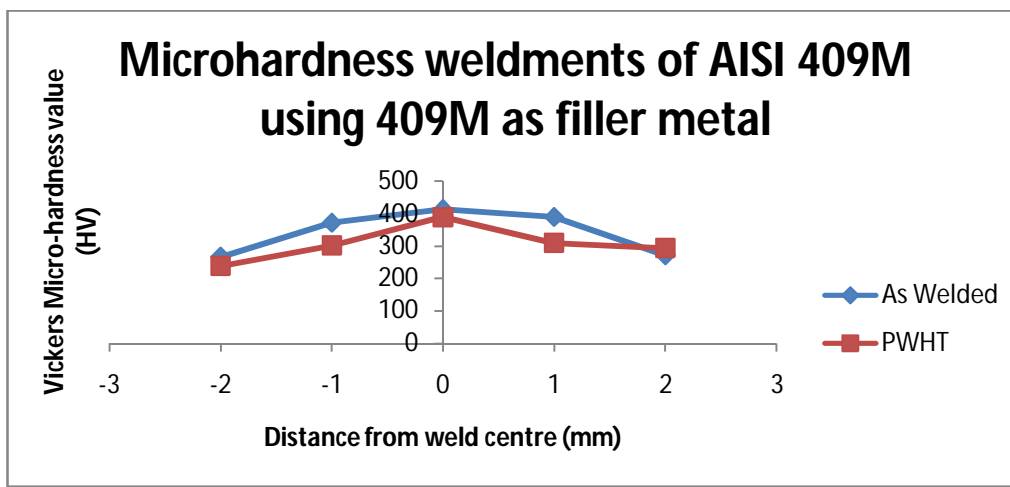


Fig. 6: Hardness Profile of GTAW Joints of SS409M Using 409M as Filler Metal.

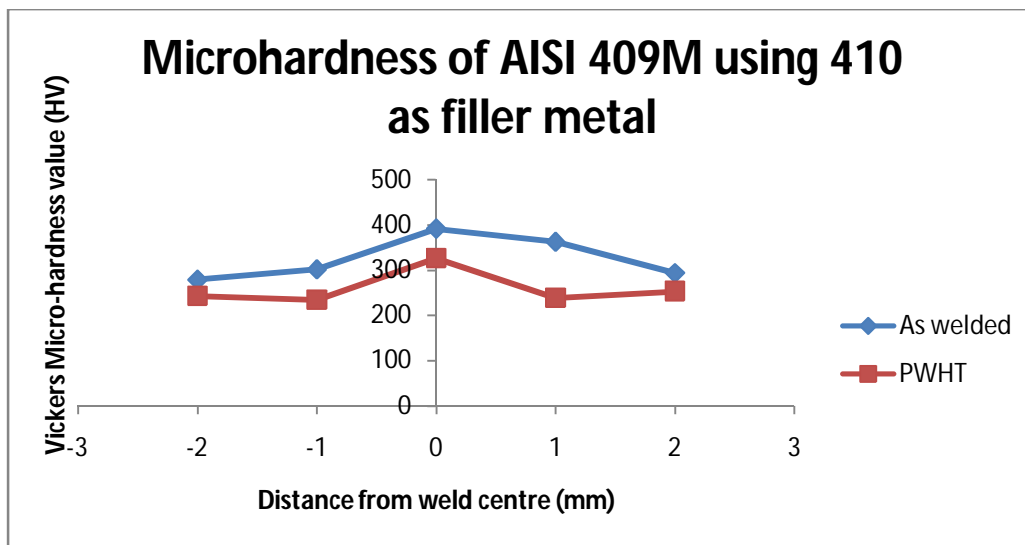


Fig. 7: Hardness Profile of GTAW Joints of SS409M Using 410 as Filler Metal.

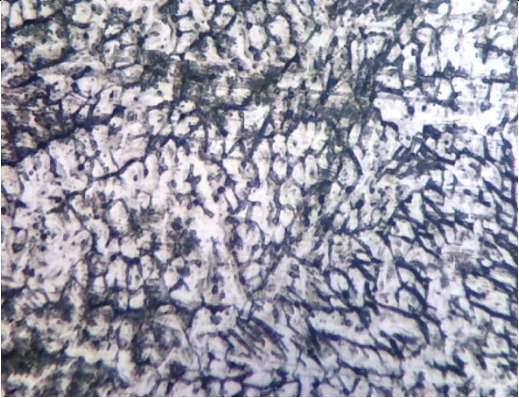
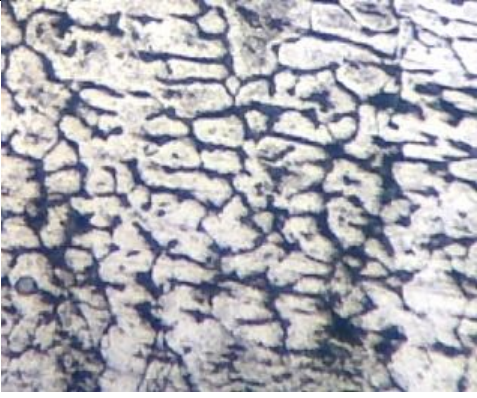
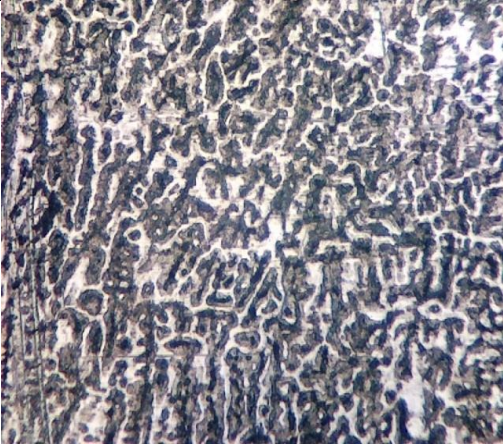
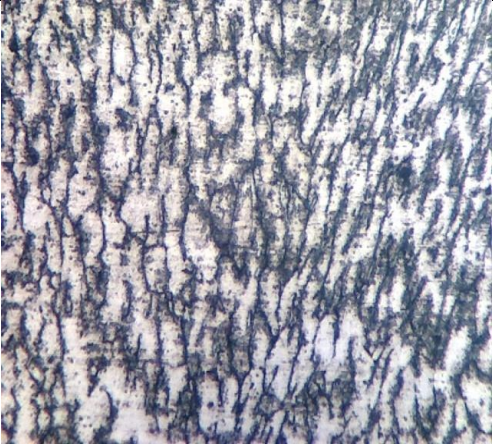
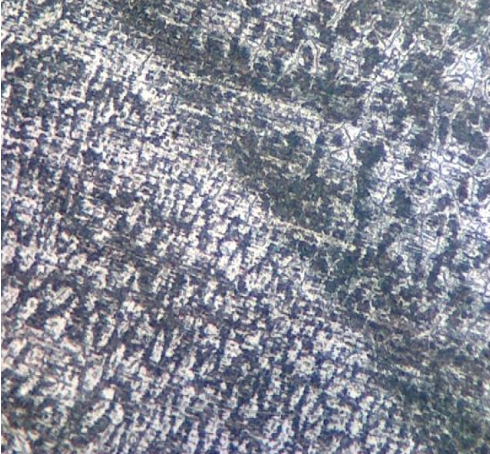
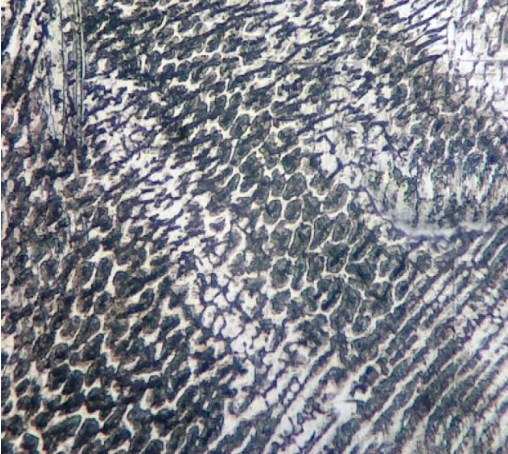
Specimen Code	As-Welded Condition	PWHT Condition
WJ ₁	 <p style="text-align: center;">(a)</p>	 <p style="text-align: center;">(b)</p>
WJ ₂	 <p style="text-align: center;">(c)</p>	 <p style="text-align: center;">(d)</p>
WJ ₃	 <p style="text-align: center;">(e)</p>	 <p style="text-align: center;">(f)</p>

Fig. 8: Optical Images of Welded Joint in As-Welded and PWHT Condition

IV. DISCUSSION

The development of austenitic structure leads to the enhancement of ductility (% of elongation) and, increases the impact toughness values. However, the development of ferritic structure improves the tensile strength. Up to some extent, strength and hardness of stainless steel will be enhanced by the formation of carbides such as chromium carbide and molybdenum carbides; higher volume fraction of these carbides will prompt lessening in ductility, strength and impact toughness. Since, there is a great extent of nickel percentage in WJ₁ which led to the improvement in ductility and impact toughness properties because of formation of fully

austenitic structure in the weld metal region as compared to the other GTA joints. On the other hand, in case of WJ₂ shows fully ferritic structure and possible formation of large volume fraction of carbides in the weld metal region and because of high amount of chromium and carbon led to the reduction in ductility and impact toughness. In case of WJ₃ there is not much extent of percentage of chromium and carbon, which led to reduction in strength and hardness properties.

Comparing the mechanical properties of PWHT samples with untreated samples, the PWHT samples showed lower tensile strength, hardness, and increase in elongation and toughness irrespective of filler metal used. After PWHT stress is relieved and a soft ferrite matrix is formed in the micro-structure of the PWHT samples because of this there is decrease in tensile strength hardness.

Optical image of WJ₁ shows that it contains solidified dendritic structure of austenite in the weld zone region. In this region it has coarse grain boundaries in as-welded condition. Optical image of WJ₂ shows the characteristics of grain boundaries with ferrite grains and presence of chromium carbides. Coarse lath ferrite structure with partially covered needle shape martensite and chromium carbides decorated the grain boundaries. It contains solidified ferrite grains in as- welded condition. In case of WJ₃, martensite lath structure is formed; this is a super saturated solution of carbon in ferrite. Grain coarsening effects are induced after PWHT irrespective of filler metals used. Due to this effect materials show ductility and toughness. After PWHT the hardness of the weld joint is decreased. PWHT induced the softness in the welded joint.

IV. CONCLUSION

Based upon the results of mechanical and metallurgical properties of GTA welded AISI 409M ferritic stainless steel joints following conclusions could be drawn

- A. Maximum UTS value of welded joints possessed by the welded joints which is fabricated with 409M filler in as welded conditions. The UTS value of WJ₂ is higher than approximately 10% compared to WJ₁, and 9% compared to WJ₃. After PWHT there was a decrease in the tensile strength irrespective of the filler metals used, it is due to the formation of soft ferrite matrix.
- B. Maximum Impact strength value possessed by the welded joints which is fabricated with 309L in as-welded conditions. The impact toughness value of WJ₁ is higher than approximately 32% compared to WJ₂ and 12% compared to WJ₃. Toughness increases due to stress relieved after PWHT irrespective of filler metals used.
- C. Hardness is lower in HAZ region compared to the weld metal irrespective of filler metals used. Very low average hardness is recorded in WJ₃ (260 VHN) as in PWHT condition and maximum average hardness is recorded in WJ₂ (342VHN) in as-welded condition.
- D. Grain coarsening effects was revealed in the microstructures images that had been taken by the optical microscope in all the welded joints after PWHT as compared to the microstructure images of welded joints in as-welded condition.

REFERENCES

- [1] Pickering F.B, Physical metallurgy of stainless steel developments. International Metals Reviews, (21) 1976: 227-68.
- [2] Sathiya, P., S. Aravindan, and A Hag Noorul. "Effect of friction welding parameters on mechanical and metallurgical properties of ferritic stainless steel." International Journal of Advanced Manufacturing Technology, (31)2007: 1086-82.
- [3] Parmar R.S Welding Processes and Technology [M]. New Delhi, Khanna Publishers, 2003.
- [4] Villafuerta, J. C. and H. W. Kerr. Grains Structures in Gas Tungsten Arc Welds of Austenitic Stainless Steel With Ferrite Primary Phase [J]. Metallurgical Transactions, 1990, 21A; 979.
- [5] Sampath, P. S., V. Manimaran, A. Gopinath and M.M. Gobisankar. "Wear and corrosion studies of ferritic stainless steel." International Journal of Research in Engineering and Technology, 4 (2015): 502-511.
- [6] Lakshminarayanan, A.K., and V. Balasubramanian. "An assessment of microstructure, hardness, tensile and impact strength of friction stir welded ferritic stainless steel joints." Materials & Design: 31(2010): 4592-4600.
- [7] Kou Sindo. Welding Metallurgy. New Jersey, A. John Wiley & Sons, INC., Publisher, 2009.
- [8] Lakshminarayanan, A. K., K. Shanmugam, and V. Balasubramanian. "Effect of autogeneous arc welding processes on tensile and impact properties of ferritic stainless steel joints." journal of iron and steel research, international: 16.1 (2009): 6216-68.
- [9] Mohandas T., G Reddy Madhusudhan, and A Mohammad Naveed. "Comparative evaluation of gas tungsten and shielded metal arc welds of a ferritic stainless steel." Journal of Material processing Technology, (94) 1999: 133-40.
- [10] Meyers A. M., and M.D. Toit. "Interstitial diffusion of carbon and nitrogen into heat-affected zones of 11-12% chromium steel welds." Welding Journal-New York-80(2001): 275-s.
- [11] Mamoru O., T. Yukito, K. Hitoshi, and F. Yuji. Development of New Steel Plates for building structural use, Nippon Steel Technical Report, 44 (1990): 8-15.



10.22214/IJRASET



45.98



IMPACT FACTOR:
7.129



IMPACT FACTOR:
7.429



INTERNATIONAL JOURNAL FOR RESEARCH

IN APPLIED SCIENCE & ENGINEERING TECHNOLOGY

Call : 08813907089  (24*7 Support on Whatsapp)